Synchronous sensing of three conserved sequences of Zika virus by a DNAs@MOF hybrid: Experimental and molecular simulation studies

Bao-Ping Xie, Gui-Hua Qiu, Bin Sun, Zi-Feng Yang, Wen-Hua Zhang,* Jin-Xiang Chen,* Zhi-Hong Jiang*

Experimental section

All reagents and solvents were obtained from commercial sources and used without further purification. Infrared (IR) spectra were recorded on a Nicolet MagNa-IR 550 infrared spectrometer. Elemental analyses for C, H, and N were performed on an EA1112 CHNS elemental analyzer. Powder X-ray diffraction (PXRD) spectra were recorded on a Rigaku D/max-2200/PC. PXRD samples were prepared by placing thin layers of samples on zero-background silicon (510) crystal plates. The X-rays generated from a sealed Cu tube was monochromated by a graphite crystal and collimated by a 0.5 mm MONOCAP ($\lambda_{Cu\text{-}K\alpha}$ = 1.54178 Å). The tube voltage and current were 40 kV and 40 mA respectively. Fluorescence spectra and anisotropy were measured on a Hitachi F-7000 spectrofluorimeter. Zeta potential measurement was carried out on a NanoZS90 zeta-sizer.

The synthesis of ligand H_2dcbbBr follows our previous report.[1] All DNA/RNA sequences were purchased from Sangon Inc (Shanghai, China) and are shown below. These samples were dissolved in DEPC H_2O and stored at −20 °C for use, and at −80 °C for long-term storage.

Target ZIKV conserved RNA sequence (T_1):

5'-CCCCAGGAGAAGCUGGGAAACCAAGCUC-3'

Complementary sequence for T_1 (probe DNA-1, P-DNA-1): 5'-

GAGCTTGGTTTCCCAGCTTCTCCTGGGG-FAM-3'

Target ZIKV conserved RNA sequence (T_2):

5′-AGCAUAUUGACGUGGGAAAGAC-3′

Complementary sequence for T_2 (probe DNA-2, P-DNA-2):

5'-GTCTTTCCCACGTCAATATGCT-ROX-3'

Target ZIKV conserved RNA sequence (T_3):

5′-GGACUAGUGGUUAGAGGAGACCC-3′

Complementary sequence for T_3 (probe DNA-1, P-DNA-1):

5'-GGGTCTCCTCTAACCACTAGTCC-Cy5-3'

Synchronous fluorescence detection of T_1, T_2, and T_3 by MOF **1**

Synchronous scanning fluorescence spectroscopy was performed with a fixed wavelength difference ($\Delta\lambda$). Fluorescence intensity at 518 nm for FAM, 604 nm for ROX, and 670 nm for Cy5 were used for quantitative analysis. These fluorescence measurements were performed at room temperature with both the excitation and emission slit width of 5.0 nm. Instruments used for the detection of RNA sequences were sterilized in an autoclavable container.

Initial fluorescence quenching experiments of P-DNAs by MOF **1** were performed by keeping the concentrations of P-DNAs constant, while gradually increasing the concentration of MOF **1**. Specifically, to a solution of the three P-DNAs with concentrations of 50 nM each in 100 nM Tris-HCl (pH 7.4, 100 mM NaCl, 5 mM $MgCl_2$) was added aliquots of a solution of MOF **1**. Fluorescence spectra were measured until saturation was observed. The quenching efficiency (Q_E) was calculated according to Eq. (1).

$$Q_E = (1 - F_M / F_0) \times 100\% \quad (1)$$

where F_M and F_0 are fluorescence intensities in the presence and absence of MOF **1**, respectively.

Subsequently, fluorescence recovery experiments were conducted at room temperature by adding target RNAs of varying concentrations to the above saturated P-DNAs@**1** solution. Fluorescence recovery efficiency was calculated according to Eq. (2).

$$R_E = F_T / F_M - 1 \quad (2)$$

where F_T and F_M are fluorescence intensities at corresponding emission in the presence and absence of RNA, respectively.

Synthesis of $[Cu(Dcbb)(bipy)(H_2O)]_n$ (**1**)

H_2dcbbBr (166.0 mg, 0.4 mmol) was suspended in H_2O (20 mL) and the pH adjusted to 7.0 with 0.1 M NaOH to give a clear solution. A H_2O (20 mL) solution of $Cu(NO_3)_2 \cdot 3H_2O$ (48.2 mg, 0.2 mmol) was then introduced and the resulting mixture stirred for 0.5 h to give a clear light green solution. A DMF (1 mL) solution of bipy (31.2 mg, 0.2 mmol) was added to give a green solution accompanied by the formation of blue precipitates. The mixture was heated at 100 ºC to yield a clear green solution and then filtered. The filtrate was allowed to stand at ambient temperature for several days to produce crystals of MOF **1**, which were collected by filtration and washed with ether and dried *in vacuo*. Anal. Calcd. for $C_{29}H_{21}CuN_4O_5 \cdot 18H_2O$: C 38.99, H 6.43, N 6.27; found: C 39.33, H 6.73, N 6.64. IR (KBr disc, cm^{-1}) *v* 3415 (s), 3104 (m), 3059 (m), 3017 (m), 2925 (m), 1668 (s), 1607 (s), 1550 (m), 1488 (w), 1411 (s), 1397 (s), 1384 (s), 1357 (s), 1327 (m), 1220 (m), 1150 (m), 1070 (m), 1019 (w), 919 (w), 875 (w), 843 (w), 817 (w), 766 (s), 720 (s), 643 (m), 604 (m).

Molecular simulation studies

The 2D structure of MOF **1**, three kinds of P-DNAs or duplex DNA@RNAs were constructed using Molecular Operating Environment (MOE) package.[2] The initial structure of P-DNAs@**1** or DNA@RNAs+**1** was manually built by placement of P-DNAs or duplex DNA@RNAs in the location 2 Å to the MOF **1** plane. Structures were first optimized in MOE using MMFF94x force field and then re-optimized in UFF of Gaussian 09 where Gibbs free energy calculations were simplified by calculating single point energies.[3] Finally, Python molecule (PyMOL) was employed for visual analysis of binding modes.[4] The binding free energy difference ($\Delta\Delta G$) between reactions of MOF **1** with single chain P-DNAs ($\Delta G_{P\text{-}DNAs@MOF}$) or double chain DNA@RNAs ($\Delta G_{DNA@RNAs+MOF}$) is evaluated according to the following Eq. (3).

$$\begin{aligned}\Delta\Delta G &= \Delta G_{P\text{-}DNAs@MOF} - \Delta G_{DNA@RNAs+MOF} \\ &= [G_{P\text{-}DNAs@MOF} - (G_{MOF} + G_{P\text{-}DNAs}) - [G_{DNA@RNAs+MOF} - (G_{MOF} + G_{DNA@RNAs})] \\ &= (G_{P\text{-}DNAs@MOF} - G_{DNA@RNAs+MOF}] - (G_{P\text{-}DNAs} - G_{DNA@RNAs}) \end{aligned} \quad (3)$$

X-ray crystallography for MOF **1**

Crystallographic measurements of MOF **1** were made on a Bruker APEX II diffractometer by using graphite-monochromated Mo Kα (λ = 0.71073 Å) irradiation. The data were corrected for Lorentz and polarization effects with the SMART suite of programs and for absorption effects with SADABS.[5] The structure was solved by direct methods and refined on F^2 by full-matrix least-squares techniques with the SHELXTL–97 program.[6] The solvent contribution was then modeled using SQUEEZE in the Platon program suite.[7] Crystallographic data have been deposited with the Cambridge Crystallographic Data Center as supplementary publication number CCDC 1568167. This data can be either obtained free of charge from the Cambridge Crystallographic Data Centre *via* www.ccdc.cam.ac.uk/data_request/cif. A summary of the key crystallographic data for MOF **1** is listed in Table S1, selected bond distances (Å) and angles (º) are shown in Table S2.

Table S1. Crystallographic data for MOF **1**.

Molecular formula	$C_{29}H_{21}CuN_4O_5$	D_{calc} (g cm^{-3})	1.038
Formula weight	569.04	λ (Mo-Kα) (Å)	0.71073
Crystal system	monoclinic	μ (cm^{-1})	0.633
Space group	$P2_1/n$	Total reflections	45620
a (Å)	13.2955(11)	Unique reflections	7998
b (Å)	17.6522(15)	No. Observations	5648
c (Å)	15.7208(13)	No. Parameters	383
α (°)	90.00	R[a]	0.0527
β (°)	99.201(2)	wR[b]	0.1482
γ (°)	90.00	GOF[c]	1.123
V (Å^3)	3642.1(5)	$\Delta\rho_{max}$ (e Å^{-3})	0.596
Z	4	$\Delta\rho_{min}$ (e Å^{-3})	-0.752
T/K	123(2)		

[a] $R = \Sigma||F_o|-|F_c|/\Sigma|F_o|$. [b] $wR = \{\Sigma w(F_o^2-F_c^2)^2/\Sigma w(F_o^2)^2\}^{1/2}$. [c] GOF = $\{\Sigma[w((F_o^2-F_c^2)^2)/(n-p)\}^{1/2}$, where n = number of reflections and p = total numbers of parameters refined.

Table S2. Selected bond distances (Å) and angles (º) for MOF $[Cu(dcbb)(bipy)(H_2O)]_n$ (**1**)

Cu(1)-O(1)	1.9326(19)	Cu(1)-O(3)#1	1.948(2)
Cu(1)-N(4)#2	2.0226(18)	Cu(1)-N(3)	2.0423(17)
Cu(1)-O(1W)	2.3169(19)	O(3)-Cu(1)#3	1.948(2)
N(4)-Cu(1)#4	2.0226(18)		
O(1)-Cu(1)-O(3)#1	174.49(7)	O(1)-Cu(1)-N(4)#2	91.55(9)
O(3)#1-Cu(1)-N(4)#2	88.17(9)	O(1)-Cu(1)-N(3)	90.56(7)
O(3)#1-Cu(1)-N(3)	90.71(8)	N(4)#2-Cu(1)-N(3)	169.45(8)
O(1)-Cu(1)-O(1W)	88.17(8)	O(3)#1-Cu(1)-O(1W)	86.38(7)
N(4)#2-Cu(1)-O(1W)	95.38(8)	N(3)-Cu(1)-O(1W)	95.02(8)

Symmetry transformations used to generate equivalent atoms: #1 $x - 1/2, -y + 3/2, z - 1/2$; #2 $x + 1/2, -y + 3/2, z - 1/2$; #3 $x + 1/2, -y + 3/2, z + 1/2$; #4 $x - 1/2, -y + 3/2, z + 1/2$.

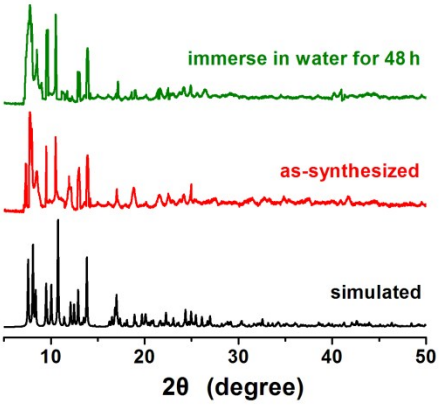

Fig. S1 PXRD patterns of MOF **1** showing the general agreement among the simulated, as-synthesized, that immersed in H_2O for 48 h.

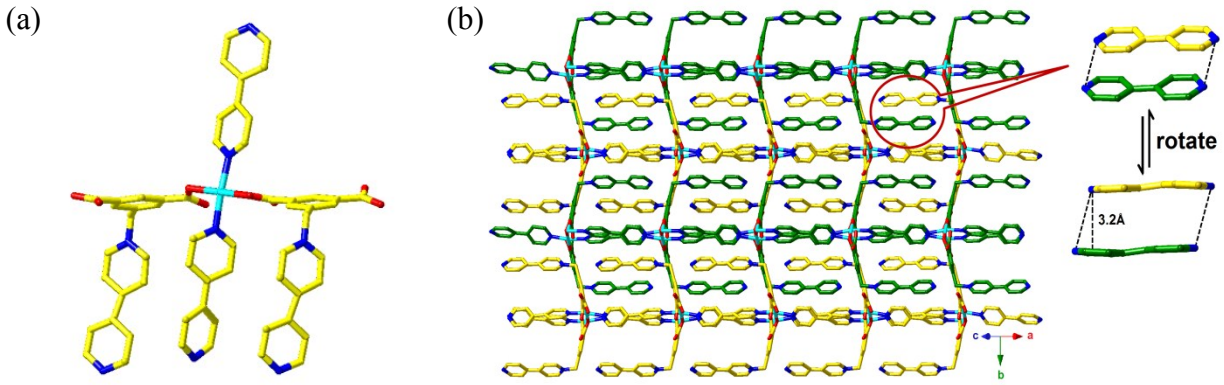

Fig. S2 (a) The coordination geometry for Cu in MOF **1**. (b) The two-dimensional structure of MOF **1**. Cu (teal), ligands (green and yellow), O (red), N (blue).

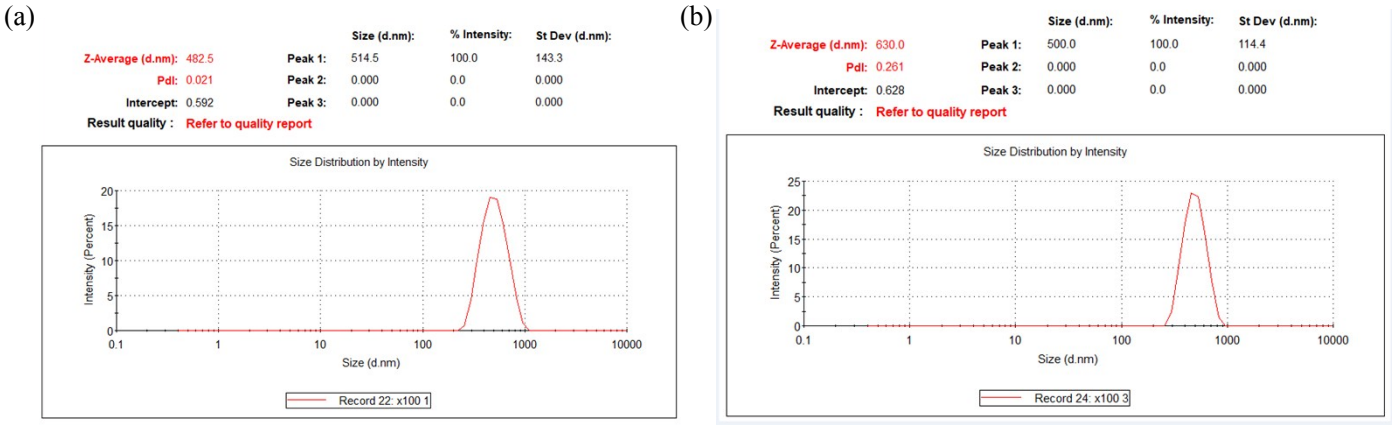

Fig. S3. DLS measurement of the MOF **1** and P-DNAs@**1**.

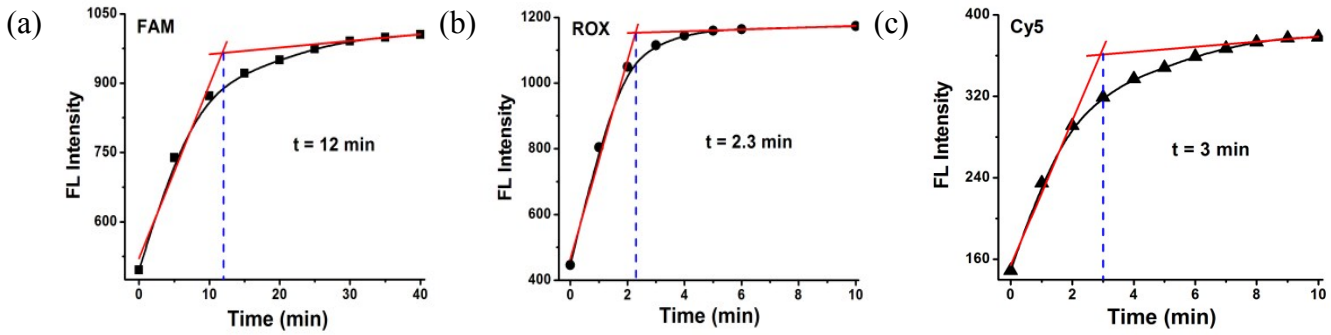

Fig. S4 Influence of incubation time between the P-DNAs@**1** and the target RNAs (25 nM) on fluorescence intensity. Concentration: all P-DNAs 50 nM, MOF **1**: 41.3 μM. The fluorescence intensity is collected at 518 nm, 604 nM and 670 nM, respectively.

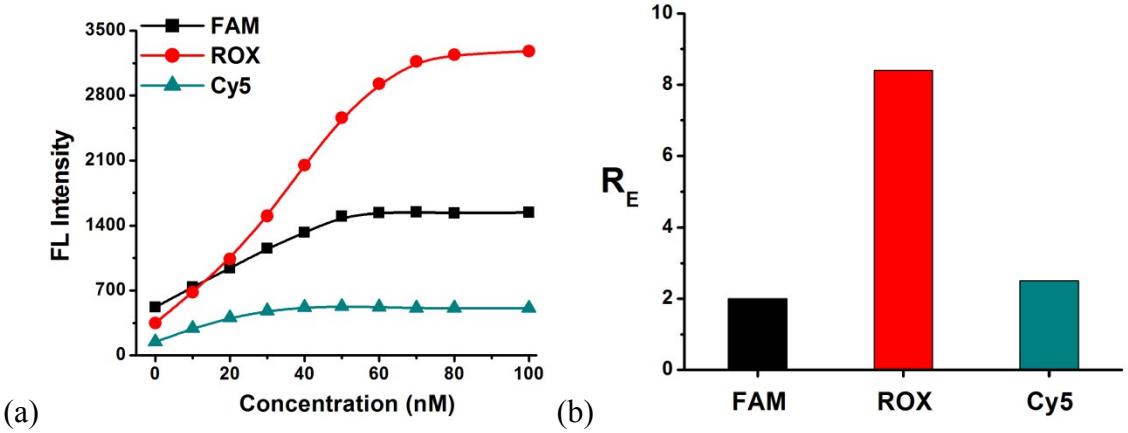

Fig. S5 (a) Fluorescence changes at 518 nm, 604 nm and 670 nm of P-DNAs versus concentrations of T_1, T_2, and T_3, respectively. (b) The recovery efficiencies R_E of P-DNAs in the presence of T_1 (50 nM), T_2 (60 nM) and T_3 (40 nM).

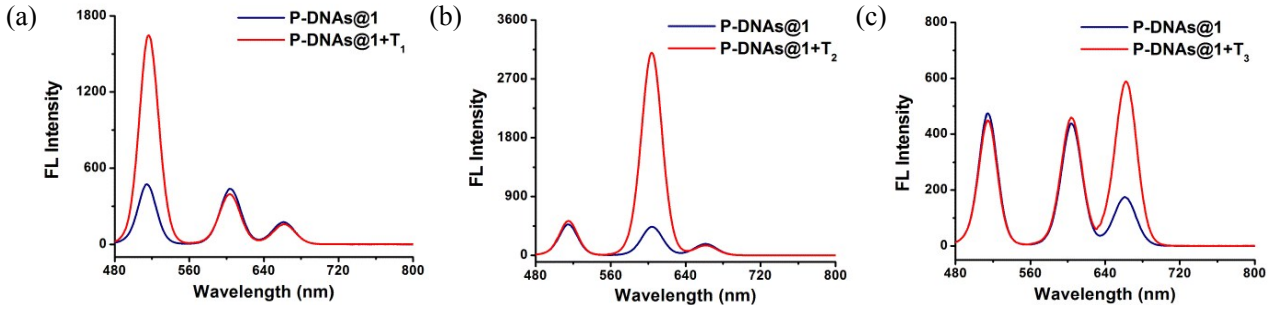

Fig. S6 Fluorescence changes of FAM, ROX and Cy5 when only T_1 (a), T_2 (b) or T_3 (c) was exclusively introduced into the P-DNAs@**1**

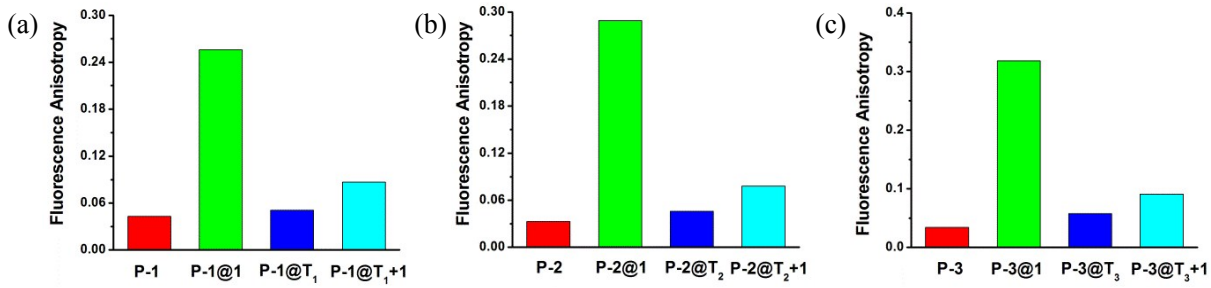

Fig. S7 Fluorescence anisotropy of P-DNA (50 nM), P-DNA@T (50 nM/50 nM) before and after the addition of MOF **1** (41.3 μM) with fluorescence incubation time of 12.0 min for P-DNA-1 (P-1) and P-DNA-1@T_1 (P-1@T_1), 2.3 min for P-DNA-2 (P-2) and P-DNA-2@T_2 (P-2@T_2), and 3.0 min for P-DNA-3 (P-3) and P-DNA-3@T_3 (P-3@T_3).

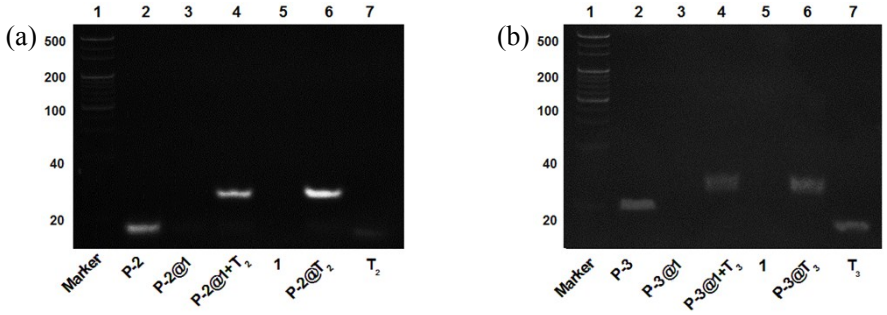

Fig. S8 Polyacrylamide gel electrophoresis of (a) P-2, P-2@**1**, P-2@**1**+T_2, MOF **1**, P-2@T_2 and T_2; (b) P-3, P-3@**1**, P-3@**1**+T_3, MOF **1**, P-3@T_3 and T_3.

References

1 J. X. Chen, H. Q. Zhao, H. H. Li, S. L. Huang, N. N. Ding, W. H. Chen, D. J. Young, W. H. Zhang and T. S. A. Hor, *CrystEngComm,* **2014**, *16*, 7722.

2 *Molecular Operating Environment (MOE)*, 2014.09; Chemical Computing Group Inc., 1010 Sherbooke St. West, Suite #910, Montreal, QC, Canada, H3A 2R7, **2014**.

3 M. J. Frisch, G. W. Trucks, H. B. Schlegel, G. E. Scuseria, M. A. Robb, J. R. Cheeseman, G. Scalmani, V. Barone, B. Mennucci, G. A. Petersson, H. Nakatsuji, M. Caricato, X. Li, H. P. Hratchian, A. F. Izmaylov, J. Bloino, G. Zheng, J. L. Sonnenberg, M. Hada, M. Ehara, K. Toyota, R. Fukuda, J. Hasegawa, M. Ishida, T. Nakajima, Y. Honda, O. Kitao, H. Nakai, T. Vreven, J. A. Montgomery Jr, J. E. Peralta, F. Ogliaro, M. Bearpark, J. J. Heyd, E. Brothers, K. N. Kudin, V. N. Staroverov, R. Kobayashi, J. Normand, K. Raghavachari, A. Rendell, J. C. Burant, S. S. Iyengar, J. Tomasi, M. Cossi, N. Rega, J. M. Millam, M. Klene, J. E. Knox, J. B. Cross, V. Bakken, C. Adamo, J. Jaramillo, R. Gomperts, R. E. Stratmann, O. Yazyev, A. J. Austin, R. Cammi, C. Pomelli, J. W. Ochterski, R. L. Martin, K. Morokuma, V. G. Zakrzewski, G. A. Voth, P. Salvador, J. J. Dannenberg, S. Dapprich, A. D. Daniels, O. Farkas, J. B. Foresman, J. V. Ortiz, J. Cioslowski and D. J. Fox, *Gaussian 09*, revision D.01; Gaussian, Inc.: Wallingford CT, **2013**.

4 Schrödinger LLC. The PyMOL molecular graphics system, version 1.8, **2015**.

5 G. M. Sheldrick, SADABS, Program for Empirical Absorption Correction of Area Detector Data; University of Göttingen: Göttingen, Germany, **1996**.

6 G. M. Sheldrick, SHELXS-97 and SHELXL-97. Programs for Crystal Structure Solution and Refinement; University of Göttingen: Göttingen, Germany, **1997**.

7 A. L. Spek, Single-crystal structure validation with the program PLATON, *J. Appl. Crystallogr.* **2003**, *36*, 7.